

Draft submitted at Zakopane Spring Seminar (1991)
Condensed Matter Studies by Nuclear Methods and to
be published by the World Scientific Publ. Co., Po Box 128,
Farrer Road, Singapore 9128.

DOE/ER/45191-19

PAC spectroscopy of electronic ceramics

DOE/ER/45191--19

DE92 014328

John A. Gardner, Ruiping Wang, and Rainer Schwenker
Department of Physics, Oregon State University, Corvallis, Oregon 97331-6507
USA

William E. Evenson
Department of Physics, Brigham Young University, Provo, Utah 84602 USA

Robert L. Rasera
Department of Physics, University of Maryland, Baltimore County, Catonsville,
Maryland 21228 USA

James A. Sommers
Teledyne Wah Chang Albany, Inc., Albany, Oregon 97321 USA

ABSTRACT

Dilute indium dopants in cerium oxides and $\text{YBa}_2\text{Cu}_3\text{O}_x$ have been studied by $^{111}\text{In}/\text{Cd}$ Perturbed Angular Correlation (PAC) spectroscopy. By controlling oxygen vacancy concentration in the cerium oxides through doping or high-temperature vacuum annealing, we have found that indium always forms a defect complex unless the sample is doped to reduce greatly the oxygen vacancy concentration. Three different vacancy-associated complexes are found with concentrations that depend on doping and oxygen stoichiometry. Another defect complex occurs in samples having negligible vacancy concentration. At low temperatures, evidence is found of interaction with an electronic hole trapped by ^{111}Cd after the radioactive decay of the ^{111}In parent. In $\text{YBa}_2\text{Cu}_3\text{O}_x$ the indium substitutes preferentially at the Y site but has measurable probability of substitution in at least one of the two copper sites. A symmetry change near 650 °C is consistent with the well-documented orthorhombic/tetragonal transition for samples in air or oxygen.

I. INTRODUCTION

Perturbed Angular Correlation (PAC) spectroscopy is an excellent technique for investigating a number of important properties of electronic ceramics.¹⁻⁴ We have used $^{111}\text{In}/\text{Cd}$ PAC to probe the structure and stability of indium donor-oxygen defect complexes in cerium oxide and have begun a study of microscopic structure of $\text{YBa}_2\text{Cu}_3\text{O}_x$. Cerium oxide has large ionic conductivity at high temperature and has great potential for technological applications. $\text{YBa}_2\text{Cu}_3\text{O}_x$ is a 90 K superconductor.

DISTRIBUTION OF THIS DOCUMENT

MASTER

DISCLAIMER

This report was prepared as an account of work sponsored by an agency of the United States Government. Neither the United States Government nor any agency thereof, nor any of their employees, makes any warranty, express or implied, or assumes any legal liability or responsibility for the accuracy, completeness, or usefulness of any information, apparatus, product, or process disclosed, or represents that its use would not infringe privately owned rights. Reference herein to any specific commercial product, process, or service by trade name, trademark, manufacturer, or otherwise does not necessarily constitute or imply its endorsement, recommendation, or favoring by the United States Government or any agency thereof. The views and opinions of authors expressed herein do not necessarily state or reflect those of the United States Government or any agency thereof.

CeO_2 is the stable oxide of cerium in air. The oxygen concentration can be decreased by annealing in a reduced oxygen pressure at high temperature. Such material has a substantial electronic and ionic conductivity.⁵⁻⁸ Ceria is often doped with trivalent (usually rare-earth) or divalent (Ca, Mg) cations. The cationic charge difference is compensated largely by oxygen vacancies, so such materials are high-temperature ionic conductors but have small electronic conductivity.⁶⁻⁸ The interaction of dopants with oxygen defects is an important topic. Our work probes complexes of (trivalent) indium dopants with oxygen defects.

CeO_2 has the cubic fluorite structure, so the electric field gradient (efg) at the Ce position in a perfect crystal will be zero. If the ^{111}Cd nucleus is substituted at a Ce site with no nearby defects, then the ^{111}Cd PAC spectrum should be unperturbed. We have investigated a number of ceria samples in which the oxygen vacancy concentration is controlled by doping or high-temperature annealing. Measurements have been made on samples held at temperatures ranging from 10 K to 1400 K, and only near the highest temperatures in this range is the PAC spectrum unperturbed. At lower temperatures, we find a variety of interactions and can identify at least four well-defined defect-associated sites. At temperatures below 500 K, we always find evidence for "aftereffects" of the ^{111}In electron capture decay.

$^{111}\text{In}/\text{Cd}$ PAC in $\text{YBa}_2\text{Cu}_3\text{O}_x$ has not been a straightforward experimental investigation. A number of groups have attempted PAC measurements⁹⁻¹⁴ and have obtained non-reproducible spectra whose interpretation has been controversial.¹⁵ Although the indium solubility in $\text{YBa}_2\text{Cu}_3\text{O}_x$ is approximately 3% per formula weight,¹⁶ it has proven extraordinarily difficult to synthesize samples in which the majority of the ^{111}In tracer is dissolved in high-quality $\text{YBa}_2\text{Cu}_3\text{O}_x$. Most of the common synthesis methods produce material in which the majority of the ^{111}In is dissolved in phases other than $\text{YBa}_2\text{Cu}_3\text{O}_x$. We have recently developed a reproducible method for making samples in which the majority of the ^{111}In is dissolved in $\text{YBa}_2\text{Cu}_3\text{O}_x$. We find that indium substitutes predominantly at the Y site but also has a substantial probability of substitution in at least one of the copper sites. We have observed the orthorhombic/tetragonal phase transition in samples heated in flowing oxygen and report preliminary data here.

II. RESULTS OF CeO_2 EXPERIMENTS

We have performed measurements over a wide temperature range on pure and lightly-doped CeO_2 samples containing trace levels (of order 10^{-9} per formula weight) of ^{111}In . Samples were made by ammonium precipitation from cerium ammonium nitrate solutions of the desired cation stoichiometry. ^{111}In in HCl solution, obtained commercially from New England Nuclear Dupont, was stirred into the solution just prior to precipitation. Samples were calcined at 1500 °C or higher for 6 hours prior to measurement. This preparation method resulted in oxide grains of order 10 microns diameter. Samples calcined below 1200 °C had much smaller grains and a significant probability that the ^{111}In was not dissolved in the bulk.

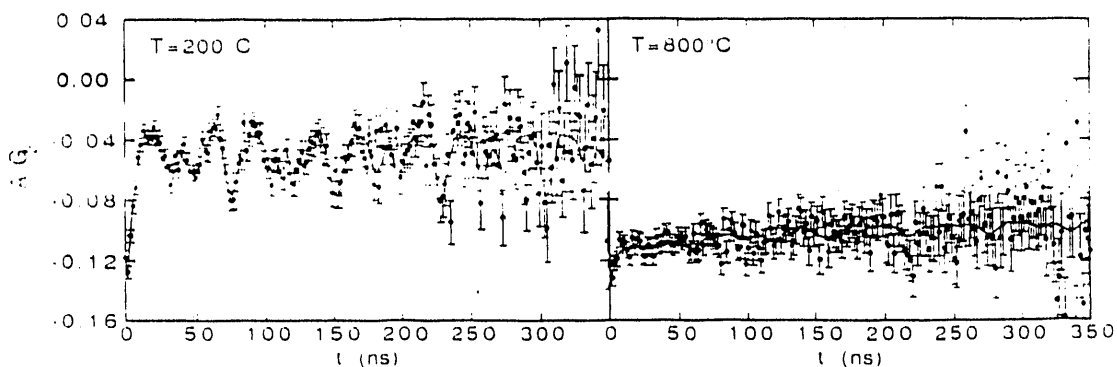


Figure 1: ^{111}Cd PAC experimental A_2G_2 spectra for cerium oxide doped with 500 ppm Nb per formula weight.

The PAC measurements were carried out using a 4-detector spectrometer with BaF_2 scintillator detectors. The apparatus is similar to one described previously.¹⁷

Figure 1 shows the experimental $A_2G_2(t)$ PAC spectra for a typical ceria sample doped with Nb, a pentavalent cation introduced to reduce the oxygen vacancy concentration to negligible levels. Below 175 K, the spectra are typical of an “aftereffects” interaction.¹⁸ $G_2(t)$ decays rapidly with time due to interaction between the Cd nucleus and an electronic hole metastably trapped after the electron capture decay of the ^{111}In parent. This interaction is not understood in detail, and we model it by a single exponential. The model is heuristic and fits the data well but not perfectly. In all cases, the experimental $G_2(t)$ does not decay exactly to zero, although the “hard core” remaining at long time is small and may be an experimental artifact.

We have made only cursory measurements below room temperature, so this region remains to be explored in future work. At and above room temperature, we find that a small fraction of the Cd nuclei are subject to a well-defined interaction with a large, asymmetric electric field gradient (efg). The relative fraction of such sites decreases with temperature and becomes negligible at temperatures of order 1000 K. The interaction frequencies are reproducible from sample to sample, but the relative fraction is not. We do not presently understand how this static interaction arises. The PAC spectrum due to the remaining ^{111}Cd nuclei can be well fitted by an exponential and a constant. The fractional weights of the exponential, constant, and static interaction contributions to the spectrum are shown in Fig. 2. The damping rate of the exponential is shown in Fig. 3(a).

It is reasonable to assume that the exponential and constant terms arise from nuclei in substitutional cerium positions in which the escape time for the trapped “aftereffects” hole is of order nanoseconds. It is straightforward to show^{19,20} that in such a case $G_2(t)$ is given by:

$$G_2(t) = \frac{r}{r + \lambda_a} + \frac{\lambda_a}{r + \lambda_a} e^{-(\lambda_a + r)t} \quad (1)$$

provided $G_2(t)$ is well-approximated by a single exponential when the hole escape

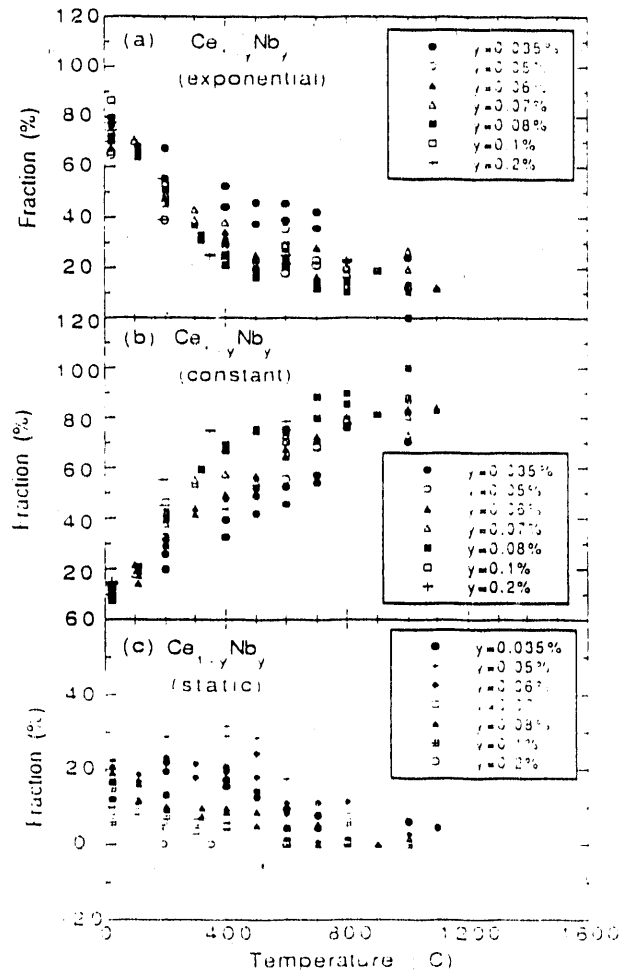


Figure 2: Fractions of (a) exponential, (b) constant, and (c) static interaction models used to fit the spectra of Nb-doped ceria at elevated temperatures.

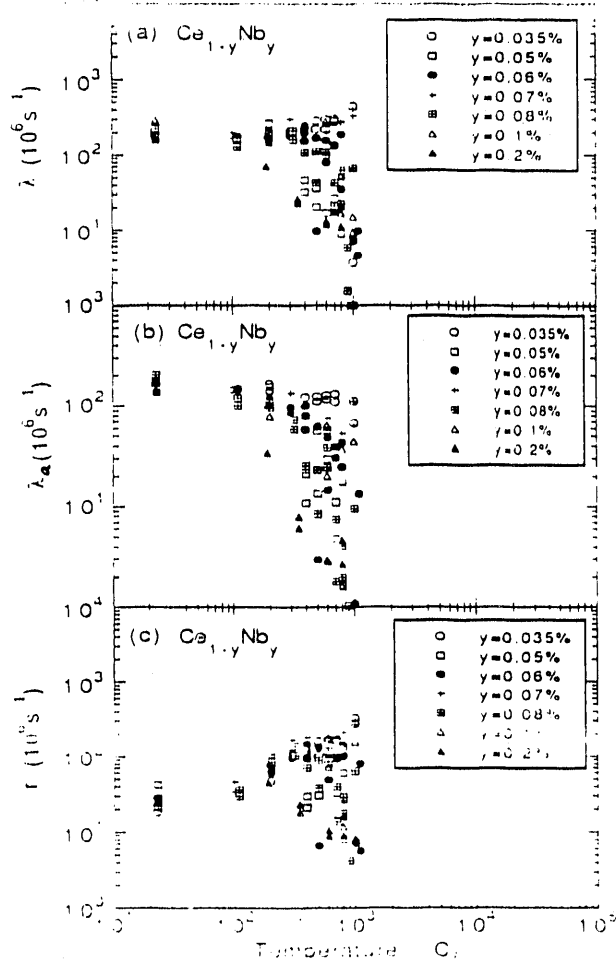


Figure 3: (a) Damping rate of the exponential model for Nb-doped ceria. (b) Exponential decay rate λ_a for ^{111}Cd PAC spectrum in presence of trapped “aftereffects” hole, and (c) escape rate r of the hole. Within this model $\lambda_a + r = \lambda$, where λ_a and r are defined by Eq. 1 in text.

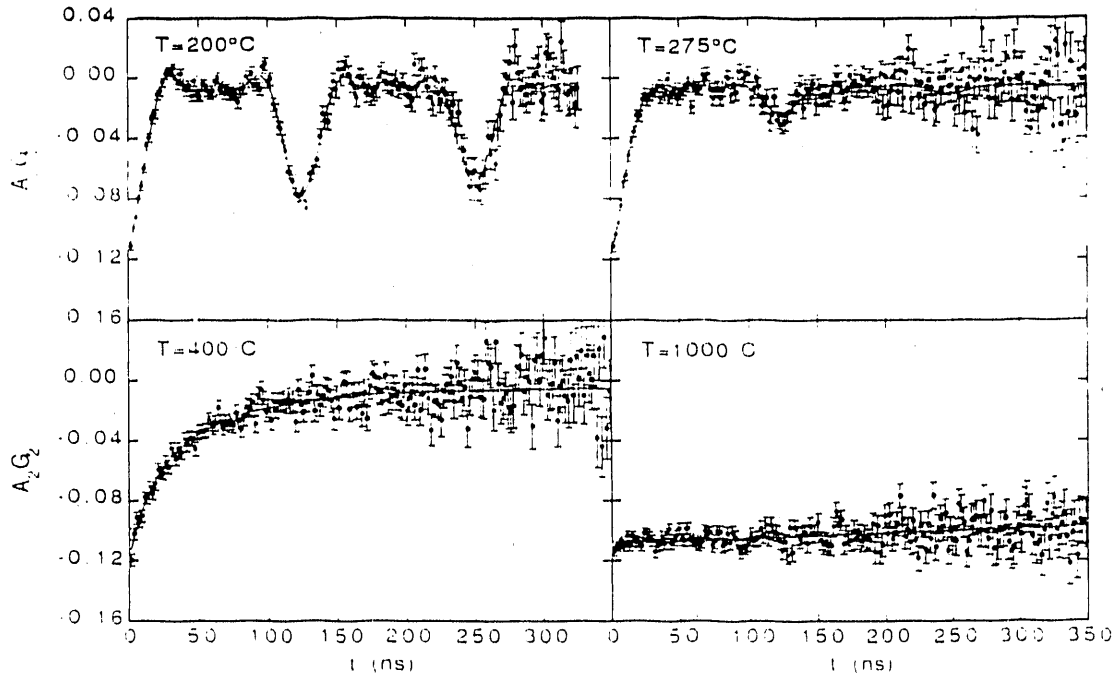


Figure 4: ^{111}Cd PAC experimental A_2G_2 spectra for undoped cerium oxide.

rate r becomes very small. The rates λ_a and r are shown in Figs. 3(b) and (c).

Spectra qualitatively similar to those of Fig. 1 are found for samples containing more than 300 ppm Nb. PAC spectra from undoped ceria are shown in Fig. 4. The spectrum at low temperature has a substantial aftereffects behavior, but almost half the ^{111}Cd nuclei are subject to a static interaction with a moderate-magnitude axially-symmetric efg. At 200 °C aftereffects are negligible, and the fraction of Cd nuclei subject to the static interaction is 100% within experimental uncertainty. We speculate that the ^{111}In parent is associated with a strongly-bound oxygen vacancy complex and that the probability of trapping a hole after ^{111}In decay is approximately 50%. Thus, at low temperature, approximately 50% of the spectrum is affected by the aftereffect interaction, but above 200 °C the hole escape rate is fast enough that its interaction with the ^{111}Cd nucleus has negligible effect on the PAC spectrum.

Figure 5 shows the Fourier transform of the 200 °C $A_2G_2(t)$ spectrum. This figure shows a frequency triplet with frequencies having ratios 1:2:3, the signature of a quadrupolar interaction with an axially-symmetric efg. At higher temperatures, the frequencies broaden, and the $A_2G_2(t)$ spectrum shows clearly that the efg is no longer static on the time scale of the intermediate state lifetime. We have examined two possibilities for the time-dependence. One possibility is that the oxygen vacancy escapes at high temperature. The second possibility is that the complex remains bound but that its symmetry axis direction changes due to thermal excitation. Detailed analysis, to be described in a later paper, clearly demonstrates that

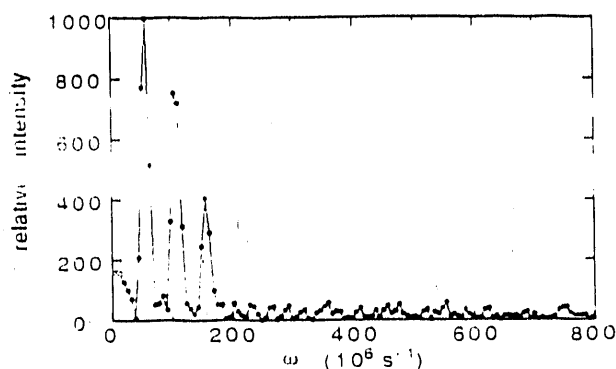


Figure 5: Fourier transform of 200 °C spectrum from Fig. 4.

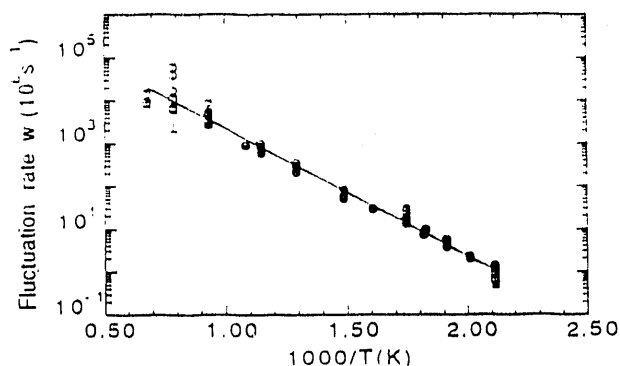


Figure 6: Single fitting parameter w vs. $1/T$. The fitting model is described in Ref. 21.

the experimental data disagree qualitatively with the first possibility but can be quantitatively explained by the second.

The random axis-reorientation hypothesis can be described accurately by a model developed by Evenson *et al.*^{21,22} We assume that the efg tensor remains constant apart from random axis reorientation at rate w . Data below 300 °C are well-represented by the “slow” limit (w/ω_Q small) of the model, whereas data above 400 °C are accurately described by the “fast” limit. The single fitting parameter w is shown vs. $1/T$ in Fig. 6. The activation energy for the axis-reorientation process is 0.6(0.2) eV. Figure 7 shows the (a) fractional weight, (b) the damping rate of the exponential decay used to approximate the “aftereffects” spectrum, and (c) the interaction frequencies ω_1 and ω_2 .

In Fig. 8(a) we show the PAC spectrum at 23 °C for an undoped ceria sample that had been annealed for 30 minutes in a mechanical pump vacuum at 900 °C and in 8(b) for a sample annealed at 1000 °C. After annealing, these samples were sealed in order to keep the oxygen vacancy concentration constant. In addition to the site seen in undoped ceria (referred to as site A), two additional sites (B and C) are

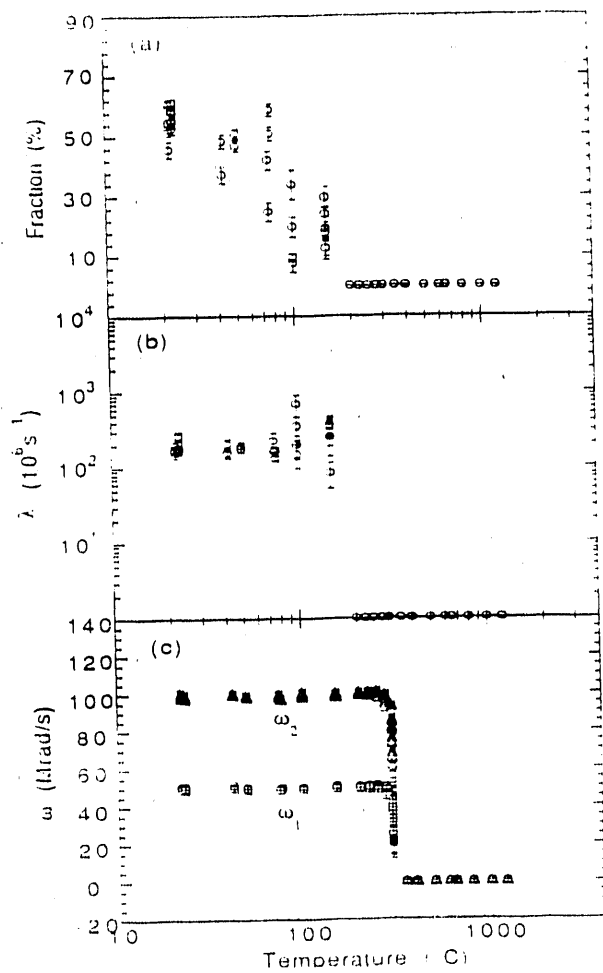


Figure 7: (a) Fraction and (b) damping rate of exponential interaction used to fit undoped ceria spectra. (c) Interaction frequencies for the A-site interaction. The quadrupole frequency $\omega_Q = 300 \times 10^6$ is obtained from fitting spectra in the static region below 300 °C and is held fixed at that value for higher temperatures.

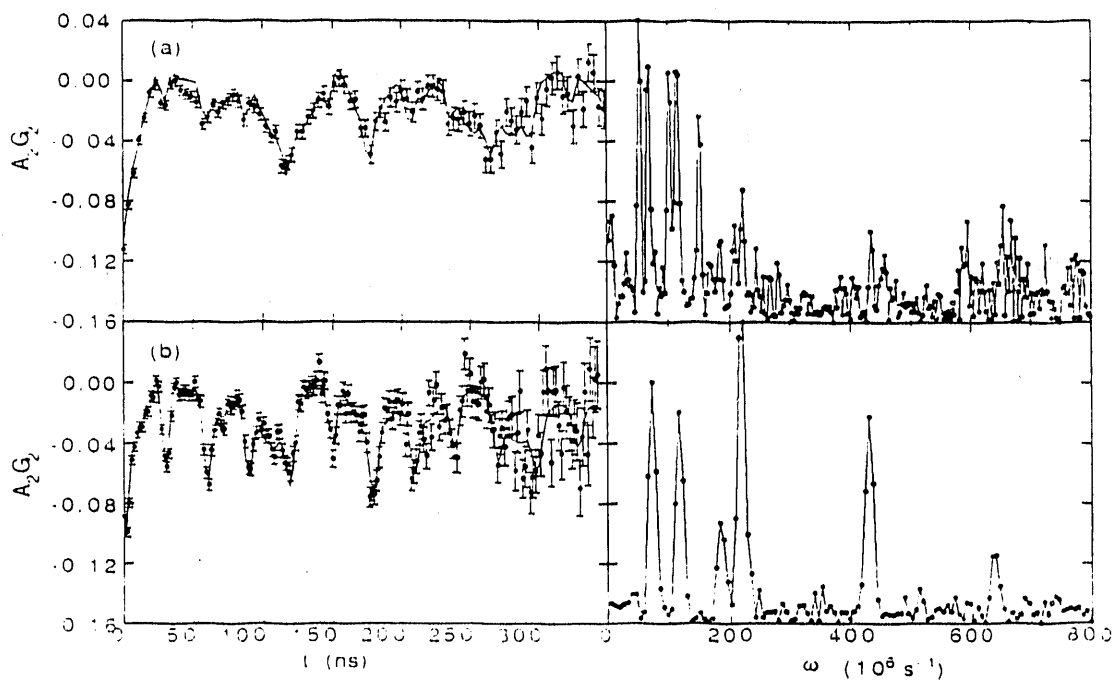


Figure 8: ^{111}Cd PAC experimental A_2G_2 spectra and Fourier transforms for undoped oxygen-depleted cerium oxide at 23 °C. (a) Sample annealed in mechanical pump vacuum at 900 °C and (b) at 1000 °C.

found. We tentatively attribute sites B and C to the presence of additional oxygen vacancies bound to the original site-A complex. The microscopic structure giving rise to these spectra has not been established unambiguously. We have speculated⁴ that site A has a missing oxygen atom next to the indium atom and that the indium atom of site C has two neighboring oxygen vacancies forming a Bevan cluster.²³

We find that PAC spectra are not strongly affected by minor contamination by rare-earth impurities that are commonly found in cerium oxides. We have used both a very high purity stock solution (cation impurities fewer than 20 ppm) and a commercial solution containing approximately 300 ppm rare-earth contaminants. No differences were found. It is interesting to note that approximately 300 ppm Nb is required to change the spectra from those of Fig. 4 to those of Fig. 1.

We have also carried out measurements of PAC spectra on samples doped with as much as 1% per formula weight of yttrium or indium. Samples doped with more than 0.4% yttrium have measureable contributions from sites of types B and C. All In-doped samples have spectra identical to those of pure ceria. These findings imply that indium does not introduce free oxygen vacancies and should therefore not yield materials with large ionic conductivity. To our knowledge, the ionic conductivity of indium-doped ceria has not been measured.

III. RESULTS OF $\text{YBa}_2\text{Cu}_3\text{O}_x$ EXPERIMENTS

We have tried a variety of sample-making techniques. Diffusion of indium into previously-synthesized $\text{YBa}_2\text{Cu}_3\text{O}_x$ was unsuccessful. The indium was apparently largely dissolved in non-representative surface layers or intergranular phases. We found very good spectra and extremely sharp Meissner flux exclusion for samples made by an evaporation method.^{13,14} Unfortunately, little indium was dissolved in the majority phase. When samples were synthesized in flowing air or oxygen, most indium dissolved in Y_2BaCuO_5 , although only a few percent of this phase was present in our samples. When samples were prepared in a restricted air flow, the indium dissolved preferentially in some other second phase whose composition we have not tried to identify. The PAC spectrum in this latter case¹³ is characterized by frequencies $\omega_1 \approx \omega_2 \approx 240 \times 10^6 \text{ s}^{-1}$. Uhrmacher¹⁵ has presented credible evidence that this particular PAC signal arises from indium substituted in an yttrium-copper oxide phase.

We have achieved better success using a sol-gel sample preparation method. An EDTA solution containing Y, Ba, and Cu in ratio 1:2:3 was prepared from high purity metal nitrates. After stirring in the appropriate amount of ^{111}In solution, the mixture was dehydrated and converted to oxides in a ceramic casserole on a hotplate. Samples were synthesized under a variety of conditions at temperatures ranging from 900 to 940 °C for times of 15 minutes to 12 hours. Some were air-quenched. Others were cooled slowly over a number of hours before being placed in the PAC spectrometer furnace. In all cases, most of the indium was dissolved in the majority $\text{YBa}_2\text{Cu}_3\text{O}_x$ phase, but no synthesis condition was found that resulted in dissolving 100% of the indium tracer.

In Fig. 9 we show ^{111}Cd PAC spectra for such samples at four different temperatures. These data were taken with a spectrometer using four NaI(Tl) scintillator detectors but otherwise similar to the apparatus used for the ceria experiments. In Fig. 10 we show the frequencies and relative fractions of two sites that we identify tentatively as indium substituted at the Y site and at the Cu-1 site in $\text{YBa}_2\text{Cu}_3\text{O}_x$. Although the exact site identification is not certain, it is unambiguously clear that the two sites are associated with $\text{YBa}_2\text{Cu}_3\text{O}_x$ and not some second phase. We base this assertion on the behavior at the melting transition. At a temperature near 1000°C in air and approximately 1030°C in flowing oxygen, $\text{YBa}_2\text{Cu}_3\text{O}_x$ decomposes into Y_2BaCuO_5 and a melt. As seen in Fig. 9, the PAC spectrum changes substantially above this temperature, with the two $\text{YBa}_2\text{Cu}_3\text{O}_x$ sites disappearing and the Y_2BaCuO_5 site becoming substantially stronger. We have also observed that the 240 Mrad signal described above persists well above the $\text{YBa}_2\text{Cu}_3\text{O}_x$ decomposition temperature. In such high temperature spectra there is also a substantial contribution from indium atoms dissolved in the melt where their average efg is zero and their contribution to $G_2(t)$ is unperturbed.

The frequencies and relative fractions of the two $\text{YBa}_2\text{Cu}_3\text{O}_x$ sites shown in Fig. 10 both change substantially in the temperature range between 600 and 750°C where the structure is known to change from orthorhombic to tetragonal. As expected, the site symmetries change from slightly asymmetric at low temperature to symmetric at high temperature. The transition region is still under investigation.

An interesting feature shown in Fig. 10 is that the site occupation probabilities change substantially above 900°C . A third site having a very large ω_1 of order $450 \times 10^6\text{s}^{-1}$ is found near 1000°C . We suspect that this may be the Cu-2 site, but further measurements on a higher-resolution spectrometer are required to test this hypothesis.

IV. ACKNOWLEDGEMENTS

We thank Mr. John Griffith and Mr. Randy Lundquist for technical assistance in data acquisition and computer analysis. We also thank Mr. Mark Preddy for his typesetting efforts. The research on cerium oxide was sponsored in part by the US Department of Energy contract DE-FG06-85ER45191. The work on $\text{YBa}_2\text{Cu}_3\text{O}_x$ was supported in part by the US National Science Foundation under contract MSM-8717809.

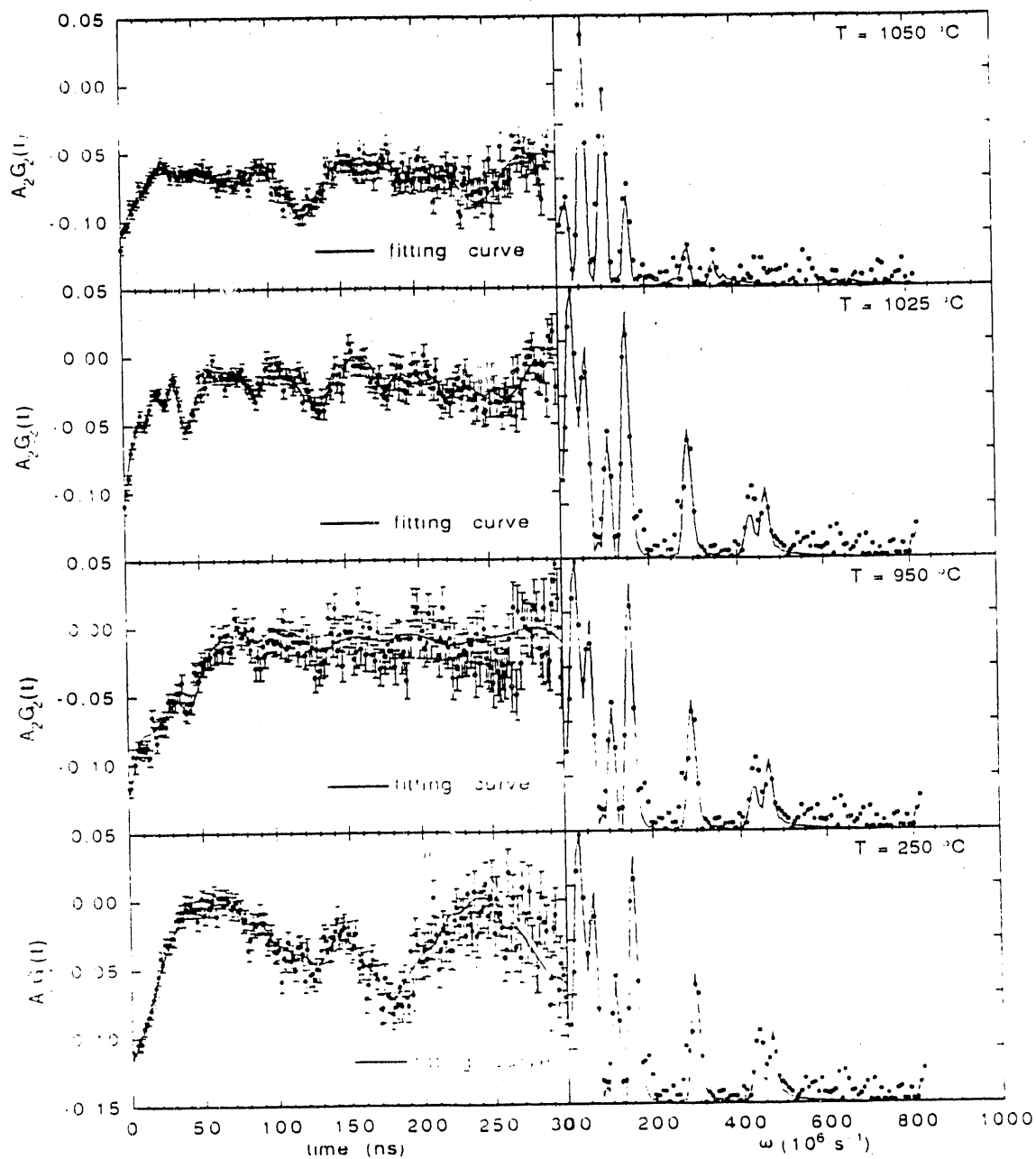


Figure 9: ^{111}Cd PAC experimental A_2G_2 spectra and Fourier transforms for sol-gel-synthesized $\text{YBa}_2\text{Cu}_3\text{O}_x$ samples held in flowing oxygen. At the lowest temperature, the material is in the orthorhombic phase, at the two higher temperatures, it is tetragonal. The highest temperature is above the decomposition temperature.

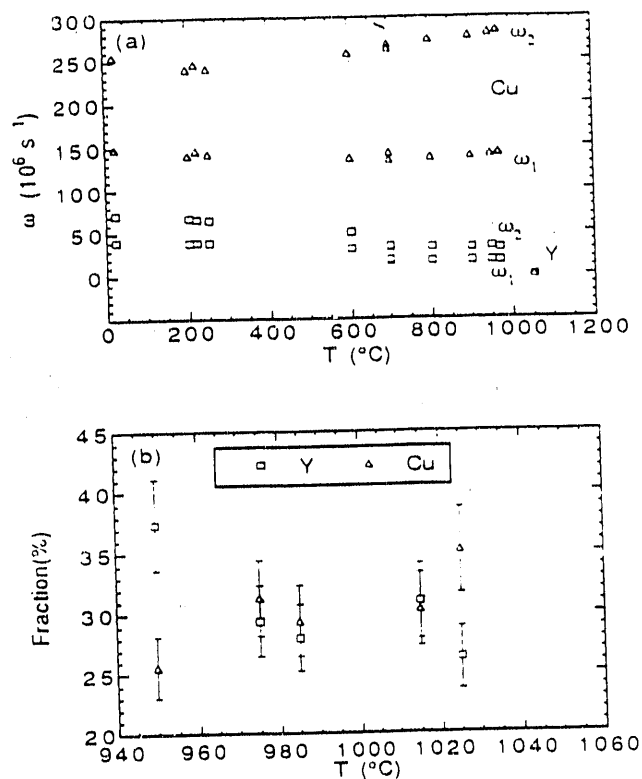


Figure 10: (a) Frequencies of sites from a representative $\text{YBa}_2\text{Cu}_3\text{O}_x$ sample. Sites labeled Y and Cu are tentatively identified as the Y and Cu-1 substitution positions in $\text{YBa}_2\text{Cu}_3\text{O}_x$. Each site is assumed to have a static efg, so spectra near the orthorhombic transition temperature were not properly fitted. (b) Fraction of the Y site and Cu-1 site in a sample for which the Y211 site fraction has a value of 20%.

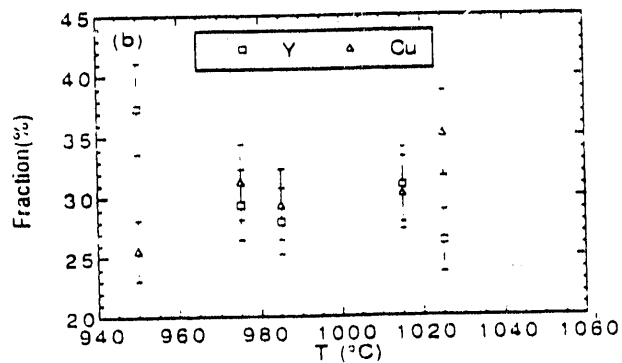
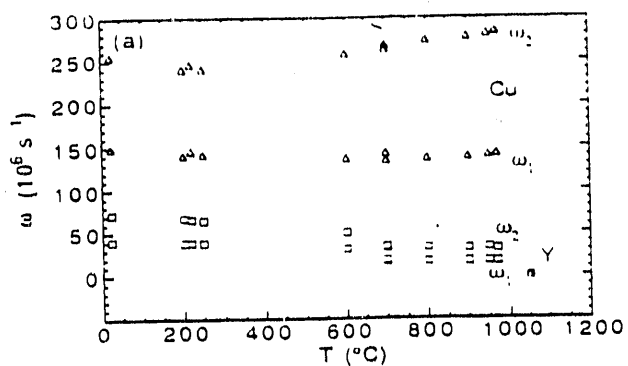


Figure 10: (a) Frequencies of sites from a representative $\text{YBa}_2\text{Cu}_3\text{O}_x$ sample. Sites labeled Y and Cu are tentatively identified as the Y and Cu-1 substitution positions in $\text{YBa}_2\text{Cu}_3\text{O}_x$. Each site is assumed to have a static efg, so spectra near the orthorhombic transition temperature were not properly fitted. (b) Fraction of the Y site and Cu-1 site in a sample for which the Y211 site fraction has a value of 20%.

References

- [1] H. Jaeger, John A. Gardner, John C. Haygarth, and R. L. Rasera, *J. Am. Ceram. Soc.* 69, 458 (1986).
- [2] J. A. Gardner, H. Jaeger, H. T. Su, and J. C. Haygarth, *Physica B* 150, 223 (1988).
- [3] H.-T. Su, R. P. Wang, H. Fuchs, J. A. Gardner, W. E. Evenson, and J. A. Sommers, *J. Am. Ceram. Soc.* 73, 3215 (1990).
- [4] R. P. Wang, J. A. Gardner, W. E. Evenson, and J. A. Sommers, paper presented at the 1991 annual meeting of the American Ceramics Society, and to be published in proceedings of the symposium on defects in oxides.
- [5] H. L. Tuller and A. S. Nowick, *J. Phys. Chem. Solids*, 38, 859 (1977).
- [6] R. Gerhardt-Anderson and A. S. Nowick, *Transport in Nonstoichiometric Compounds*, edited by G. Simkovich, (Plenum Press, New York, 1985).
- [7] D. Y. Wang and A. S. Nowick, *J. Phys. Chem. Solids*, 77, 639 (1983).
- [8] R. Gerhardt, W.-K. Lee, and A. S. Nowick, *J. Phys. Chem. Solids* 48, 563 (1987).
- [9] M. Uhrmacher and A. Bartos, paper presented at the Eighth International Conference on Hyperfine Interactions, Prague, 1989, to be published in conference proceedings issue of Hyperfine Interactions.
- [10] H. Plank, F. Meyer, and W. Witthuhn, *Phys. Lett.* A133, 451 (1988).
- [11] P. Singh, M. N. Nyayate, S. H. Devare, and H. G. Devare, *Phys. Rev. B* 39, 2308 (1989).
- [12] G. L. Catchen, M. Blazskiewicz, A. J. Baratta and W. Huebner, *Phys. Rev. B* 38, 2824 (1988).
- [13] H. T. Su, A. G. McKale, S. S. Kao, L. L. Peng, W. H. Warnes, John A. Gardner, and J. A. Sommers, *Ceramic Superconductors II*, (American Ceramic Society, Westerville, Ohio, 1988).
- [14] J. A. Gardner, H. T. Su, A. G. McKale, S. S. Kao, L. L. Peng, W. H. Warnes, J. A. Sommers, K. Athreya, H. Franzen, and S.-J. Kim, *Phys. Rev. B* 38, 11317 (1988).
- [15] M. Uhrmacher and A. Bartos, *Hyperfine Interactions* 61, 1073 (1990).

- [16] G. Weidlich, M. Goelz, R. P. Wang, W. E. Evenson, J. A. Gardner, D. A. Keszler, J. A. Sommers, and J. E. Ostenson, *J. Mater. Res.* 6, 446 (1991).
- [17] H. Jaeger, J. A. Gardner, H. T. Su, and R. L. Raseria, *Review of Scientific Instruments.* 58, 1694 (1987).
- [18] A. G. Bibiloni, C. P. Massolo, J. Desimoni, L. A. Mendoza-Zélis, F. H. Sánchez, A. F. Pasquevich, L. Damonte, and A. R. López-García, *Phys. Rev. B* 32, 2393 (1985).
- [19] A. G. Bibiloni, J. Desimoni, C. P. Massolo, L. A. Mendoza-Zélis, A. F. Pasquevich, F. H. Sánchez, and A. R. López-García, *Phys. Rev. B* 29, 1109 (1984).
- [20] R. P. Wang, PhD thesis, Oregon State University, 1991, (unpublished).
- [21] W. E. Evenson, A. G. McKale, H. T. Su, and J. A. Gardner, *Hyperfine Interactions* 61, 1379 (1990).
- [22] W. E. Evenson, J. A. Gardner, R. P. Wang, H.-T. Su, and A. G. McKale, submitted to *Hyperfine Interactions*, July, 1990.
- [23] D. J. M. Bevan and J. Kordis, *J. Inorg. Nucl. Chem.* 26, 1509 (1964).

**DATE
FILMED**

7 / 9 / 92

